

Sensitivity of different convective parameterization schemes on tropical cyclone prediction using a mesoscale model

Saji Mohandas · Raghavendra Ashrit

Received: 30 May 2012 / Accepted: 5 August 2013 / Published online: 13 April 2014
© Springer Science+Business Media Dordrecht 2014

Abstract This study presents an intercomparison of four cumulus parameterization schemes (CPS) in the prediction of three cases of tropical cyclones in the north Indian Ocean. The study makes use of the Weather Research and Forecasting model of Non-hydrostatic Mesoscale Model version with a horizontal resolution of 27 km. The four deep cumulus schemes studied are (a) modified Kain–Fritsch (KF), (b) Betts–Miller–Janjic, (c) Simplified Arakawa–Schubert and (d) Grell–Devenyi Ensemble (GD) schemes. Three cases chosen for the study are unique cases with entirely different characteristics, synoptic/convective conditions and with varying levels of performance of the driving global model forecasts. The objective of the current study is to report the relative performance of the CPSs rather than the accuracy of the forecasts, under different convective conditions as reflected in the initial and boundary conditions. The study shows that generally KF scheme produced near-realistic track, intensification and the associated rainfall patterns and GD performed worst in terms of convective organisation and the sustained intensity. The impact of cumulus parameterization schemes and its performance vary widely among the three cases studied. The standard verification scores and the contribution of grid-scale precipitation towards the total rainfall by the mesoscale model are also compared between the different cases as well as the different cumulus parameterization schemes. The performance evaluation of the tropical cyclone predictions by the mesoscale model is influenced by not only the model physics but also the convective conditions as input into the model.

Keywords Cumulus parameterization · Tropical cyclones · Weather Research Forecasting model · Convective conditions

S. Mohandas (✉) · R. Ashrit
National Centre for Medium Range Weather Forecasting, A-50, Sector-62, Noida, India
e-mail: sajimd@yahoo.com; saji@ncmrwf.gov.in

1 Introduction

Tropical cyclones are one of the extreme manifestations of multi-scale organized convection in tropics, with many complex interactions between ocean, land surface, planetary boundary layer (PBL) and convective processes. Insufficient understanding and lack of observational data sets limit our ability to properly represent the convective processes as well as their organization in all time and space scales. Some of the main challenges of the cumulus parameterization problem lie in the realistic representation of the resolved and subgrid scale precipitation and the dependencies of the same on the resolution of the numerical model used for the simulations. Several questions being addressed are related to how well certain parameterization schemes perform under a variety of convective conditions and with the increase in the resolution of the mesoscale models. There are systematic studies comparing the performance of deep convective parameterization schemes in high-resolution Fifth-generation NCAR/Penstate Mesoscale Model (MM5) or Weather Research and Forecasting (WRF) models (Wang and Seaman 1997; Ma and Tan 2009; Yang and Tung 2003; Stensrud et al. 2000; Davis et al. 2010; Gopalakrishnan et al. 2012; Gentry and Lackmann 2010; Wang 2012; Nasrollahi et al. 2012). There are many studies using mesoscale models on the prediction of tropical cyclones or extreme rainfall events over Indian region (Rao and Prasad 2007; Vaidya 2007; Vaidya and Kulkarni 2007; Deb et al. 2008; Litta et al. 2011; Singh et al. 2011).

There are a wide variety of cumulus parameterization schemes (CPS) that are developed and tested for limited number of convective environments and horizontal resolutions (Kuo et al. 1996; Gallus 1999; Peng and Tsuboki 1997; Yang et al. 2000; Spencer and Stensrud 1998). A focused study on the sensitivity of these schemes on the behaviour of the Indian Ocean tropical cyclone (TC) forecasts for a particular scale and a particular resolution is attempted here. Among the systems formed and developed into TC, three cases of TC which sustained their intensity for at least 4 or 5 days have been selected for the current study. They are Gonu (1–7 June, 2007), Sidr (10–16, November, 2007) and Nargis (26 April–3 May, 2008). Some examples of studies related to these TC systems are Deb et al. (2010), Akter and Tsuboki (2012), Rafy and Hafez (2008) and Lisan and McPhaden (2011). Section 2 describes the methodology and the data used.

Roy and Kovordanyi (2012), in a review on TC track forecasts, state that difficulties in accurate cyclone forecasts arise because the geographical and climatological characteristics of the various cyclone formation basins are not similar. Variables like precipitable water, lower and upper level velocities, location of jet streaks, temperature advection and upper level vertical velocities can all affect storm strength, movement and precipitation rate in a synoptically forced environment (Aylward and Dyer 2010; Schumacher and Johnson 2005). Chen et al. (2010) studied the steering and onset mechanisms of twin Philippine tropical cyclones, which occurred in May 2008, soon after the formation of TC Nargis over the Indian Ocean basins. They found out the effects of the synoptic interaction between the tropics and the midlatitudes through the spinup of the monsoon cyclonic shear flow as one of the reasons of TC genesis. Gopalakrishnan et al. (2012) opined that forecasting the TC intensity for initially weak storms poses major problems due to artificial effects of the bogus vortex during the initialization process. There are several studies on the probabilistic and climatological aspects favourable for TC genesis over Indian Ocean basins (see Belanger et al. 2012; Evan and Camargo 2011; Gray 1968). Evan and Camargo (2011) attempted to understand the relationship between Arabian Sea cyclonic storms and their large-scale environment. They demonstrated how the seasonal cycle in TC activity is a function of the state of the coupled low-level winds and surface ocean temperature,

relative vorticity, vertical wind shear and 200-hPa winds. May storms are normally associated with an early southwest monsoon onset. June storms are associated with conditions consistent with a delayed monsoon onset. November storms are associated with sea level pressure anomalies over Bay of Bengal.

The current study deals with the associated characteristics of the TC forecasts in relation to the CPSs, which is the only difference between the set of experiments. Model performance is assessed in terms of track error and intensity prediction. Though the explicit simulation of individual cloud cells requires a resolution of the order of at least a few hundred metres, some gross dynamic features associated with the mesoscale convective systems (MCS) can be identified using models with a resolution of a few tens of kilometers. Gentry and Lackmann (2010), while studying the sensitivity of TC intensity and structure on the horizontal grid spacing of grid lengths between 8 and 1 km, made some suggestions on the optimal grid spacings. They suggested a grid spacing of 2 km or less in the representation of important physical processes in TC eyewall. Wang and Seaman (1997) tested the hybrid schemes (with both parameterized and grid-scale convection) as well as only explicit scheme in their studies with WRF model for separating the effect of explicit simulation at 15 km resolution. They found generally good skill for precipitation forecast for the areal coverage for only explicit (grid-scale) convection in cold season experiments. Under the influence of strong large-scale forcing in a relatively stable atmosphere and with ample moisture, grid-scale vertical motion may often be sufficient to lift the moist air and produce precipitation. In warm season experiments, where the large-scale dynamic forcing is weak and the convection initiation is in serious error, they found a greater scatter among the skill of different CPSs. It is not clear from the experiments with hybrid schemes that whether the parameterized physics can correct the subsequent evolution and structure of the convective system. Similar conclusions have been drawn by the study by Yang and Tung (2003) for Taiwan.

A reasonable partition between the subgrid-scale and resolvable rainfall is crucial to produce realistic representation of precipitation events (Houze 1997; Wang 2012; Akter and Tsuboki 2012). Over two-thirds of MCS rainfall is convective as opposed to stratiform (Houze 1977; Johnson and Hamilton 1988), and the deep convective representation must be able to realistically estimate not only the convective rainfall but also the feedbacks on the surrounding environment that influence further convective development (Molinari and Dudek 1992). Established studies of observed mesoscale phenomena indicate that parameterized, moist downdrafts are crucial for reproducing many of the observed mesoscale characteristics as well as correct large-scale temperature fields (Cram et al. 1992; Zheng et al. 1995; Stensrud and Fritsch 1994; Chen et al. 2012; Krikken and Steenveld 2012). Also in some precipitation events, the characteristics of the precipitation can transform from predominantly convective to a resolvable mesoscale system as the systems mature (Dudhia 1989; Zhang 1989; Zhang et al. 1989). Akter and Tsuboki (2012) reported that the strong outer rainbands to the east of TC centre of TC Sidr consisted of convection with stratiform only in the downwind portion of the band and the upwind and middle portion contained active convective cells without stratiform rain.

Wang (2012) examined the balanced response to convective and stratiform heating rates at the pregenesis stage of a hurricane. They reported that compared to the convective heating rate, the stratiform heating rate has a weaker magnitude and smaller radial and vertical gradients. Houze (1997) mentioned ‘Convective/Stratiform separation’ as the separation of the convective component of the precipitation. In a deep precipitating tropical cloud system, the stratiform precipitation region is typically a region of older convection. He stated that it is important to separate the convective precipitation from all the rest as the

microphysical growth processes are different in convective precipitation areas (coalescence/riming) from those in the stratiform and intermediary areas (vapour diffusion). As the region of convective cells weakens, the large-scale mass field response changes to a layered structure with lower atmosphere dominated by downdrafts and the upper levels by weak updrafts. Thus, the relative contributions of convective and non-convective parts of the model rainfall output are also examined. At different stages of prediction and at different stages of cyclone development, these characteristics are found to vary widely with the CPSs as well as with case-to-case, which in turn represent the different convective conditions and the quality of initial and boundary conditions provided by the driving global model. The objective of the current study is to present the relative performance of the CPSs under different convective environments. A brief description of the synoptic conditions is given in Sect. 3, and the last two sections deal with the results and summary, respectively.

2 Data and methodology

Weather Research and Forecasting model of Non-hydrostatic Mesoscale Model flavour (WRF NMM SI version 2.2) is used for testing three cases and four CPSs. Analysis and forecasts of T254L64 global spectral model (Rajagopal et al. 2007) are used for the initial and boundary conditions as well as for verification. Tropical rainfall measuring mission (TRMM)-derived daily rainfall estimates are used for rainfall verification, which is the best reliable source over the oceanic areas (Simpson et al. 1996). Marchok et al. (2007) suggested a scheme for validating the quantitative precipitation forecasts in terms of the ability to match the observed rainfall patterns, the ability to match the mean value and the volume of the observed rainfall and the ability to produce the extreme amounts often observed in tropical cyclones. The verification statistics in the current study were generated not strictly following a similar principle of track-relative analysis, but after taking out a domain of 10×10 degree box centred around the estimated forecast locations of TCs. Thus, the intent is to study the associated rainfall characteristics only rather than verification over the entire domain of integration. This strategy of verification does not ensure that the associated rainfall region is exactly superposed over the observed satellite-derived precipitation region during comparisons between the two. There can be instances when the entire pattern of observed rainfall can be partly or fully out of the domain of verification for a particular case or CPS, reducing the skill score drastically. Average of all the skill scores will be mostly very much less than the individual cases or with different initial conditions (ICs).

The deep convective schemes used are modified Kain–Fritsch (KF: Kain 2004; Kain and Fritsch 1990, 1993), Betts–Miller–Janjic (BMJ: Betts and Miller 1993; Janjic 1994, 2000), Simplified Arakawa–Schubert (SAS: Pan and Wu 1995; Grell 1993; Grell et al. 1994) and Grell–Devenyi Ensemble scheme (GD: Grell and Devenyi 2002). Kain–Fritsch convective parameterization (Kain and Fritsch 1990, 1993) is based on an entraining/detraining plume model that removes all available buoyant energy in a convective time period. It includes downdrafts and was designed to parameterize convection in models with a horizontal grid spacing of approximately 20–30 km. Simplified Arakawa–Schubert convective parameterization is based on a quasi-equilibrium, single-cloud model and was designed for models with a horizontal grid separation in the 10–30 km range. Penetrative convection is based on Arakawa and Schubert (1974) as simplified by Grell (1993) and with a saturated downdraft. A major simplification of the original Arakawa–Schubert scheme is to consider only the deepest cloud and not the spectrum of clouds. Betts–Miller–Janjic convective parameterization is derived from the scheme originally developed by

Betts and Miller (1993) but incorporates several important differences summarized in Janjic (2000). BMJ is a relaxation scheme that adjusts the atmosphere to a reference, post-convective thermodynamic profile based on a non-dimensional quantity called the cloud efficiency (Janjic 1994) and does not include explicit downdrafts. BMJ has been used successfully in mesoscale models that have a grid spacing ranging from around 10 to more than 50 km. The Grell-Devenyi Ensemble scheme is an expansion from the Grell convective parameterization (Grell 1993) to include several alternative closure assumptions that are commonly used in convective parameterizations. These assumptions, rooted in various considerations of convection initiation and development, represent a natural span of uncertainties in convective parameterization. The unique aspect of the GD scheme is that it uses 16 ensemble members derived from 5 popular closure assumptions to obtain an ensemble-mean realization at a time and location. This is used operationally at 20 km resolution (Grell and Devenyi 2001).

Apart from difference in convective parameterization schemes, the model experiments were carried out with identical configurations. All the experiments used common initial and boundary conditions. The domain is approximately 40–120°E and 15°S–45°N. Fig. 1 shows the orography. Table 1 describes the list of other physics options employed. No tuning of parameters was done to enhance its performance in any particular case. WRF NMM is run for 3 days at a resolution of 27 km in the horizontal and 38 vertical levels with initial and boundary conditions interpolated from National Centre for Medium Range Weather Forecasting (NCMRWF) T254L64 model analyses and forecasts. All experimental runs are carried out without any mesoscale data assimilation or nudging. The number of initial conditions used for the experiments are 5 (1–5 June, 2007) for Gonu, 4 (11–14 November, 2007) for Sidr and 6 (27 April–2 May, 2008) for Nargis case as these are the dates for which corresponding track positions are available from India Meteorological Department (IMD), and the statistics are prepared with locations of systems at every 24-h intervals with respect to IMD positions.

For all the three cases, the total sample size of integrations is 15, and for each field at each grid point, the values were taken at 24-hour interval making a total of 15 analyses and 45 forecast values. The simulated prognostic fields of wind, minimum sea level pressure (SLP) and rainfall were verified against the analyses or observed estimates. The 24-h accumulated rainfall forecasts were evaluated against the TRMM rainfall estimates quantitatively using statistical skill scores (Bias Score BS, Threat Score TS and Equitable Threat Score ETS) with the threshold values of 1, 10, 20... up to 90 mm. Also, the percentage contribution of non-convective precipitation over the total precipitation was also computed for each day of forecasts along with the averages. As the study looks into the aspects related to the different convective conditions, the composite average of all the statistics was presented for total, casewise, CPS-specific etc.

3 Case description

The three systems selected for the study show distinct characteristics in genesis and movement. The tropical cyclone Gonu developed as a depression over the east central Arabian Sea on 1 June, 2007. It moved mainly westwards and northwestwards, ultimately intensifying into a super cyclonic storm and crossed the Makran coast on 7 June, 2007, as a cyclonic storm. The minimum SLP reported is 920.0 hPa at 15z on 4th June, 2007, with an estimated maximum wind speed of 127 Kts. The Tropical cyclone Sidr developed over southeast Bay of Bengal as a depression on 12 November, 2007, mainly moving

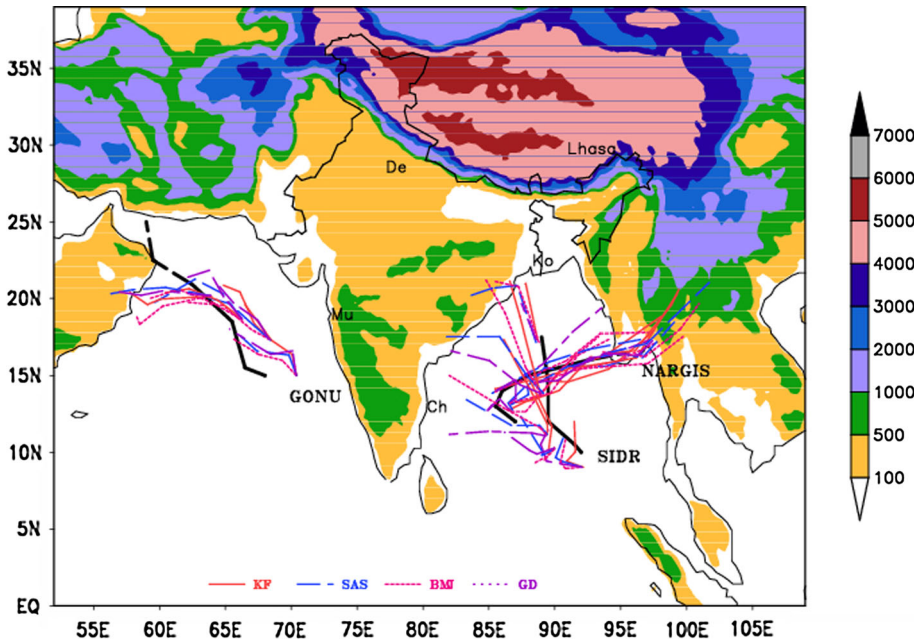


Fig. 1 Weather Research and Forecasting model of Non-hydrostatic Mesoscale Model (WRF NMM) orography in metres and the observed (*thick lines*) and forecast tracks of Gonu, Nargis and Sidr for total 15 initial conditions

Table 1 Brief description of WRF NMM model

Horizontal resolution: 0.24 degree (appr:27 km), vertical: 38 levels, grid size: 160 × 250

Time-step: 60 s

Land surface model : NOAH LSM with 4 soil levels

Surface layer : Monin–Obukhov (Janjic)

Planetary boundary layer scheme : Mellor–Yamada–Janjic TKE

Longwave radiation : GFDL (Eta)—invoked 3 hourly

Shortwave radiation : GFDL (Eta)—invoked 3 hourly

Microphysics: Ferrier (new Eta)

Deep convection: Kain–Fritsch (new Eta)

northwestwards and northwards, crossed Bangladesh in the evening of 15 November, 2007. The minimum SLP was 944.0 hPa on 15th November with a maximum wind speed estimated to be 115Kts. The tropical cyclone Nargis also developed over south central Bay of Bengal by 27 April, 2008, and initially moved northwestwards till 28th, thereafter northwards. By 30th, it recurved and moved northeastwards, intensifying and reaching Myanmar coast by 2 May, 2008. It crossed the coast on 2 May, 2008 and thereafter moved east northeastwards, weakening by 3 May, 2008. On 2nd May, 2008, it attained a minimum SLP value of 962.0 hPa and a maximum wind speed estimates of 90 Kts.

Yang et al. (2000) suggested that the synoptic or mesoscale environment provides the primary control on the model's rainfall forecast skill and the CPSs used in the model only slightly modify the forecasts at the grid distance of 15 km. They demonstrated the

variability in rainfall forecasts, both due to different CPSs and various synoptic forcings, which will confront the forecaster in their daily operations. The three TCs considered for the present study formed in three different seasons. Gonu developed during the monsoon onset period, delaying the onset of Monsoon 2007 and is a rare case of supercyclone developed over Arabian Sea basin. Sidr formed over South Bay of Bengal during the post-monsoon period and Nargis formed over southeast Bay of Bengal during the pre-monsoon period. All of them have origins in different ocean basins or seasons and followed totally distinct tracks and landfall patterns; Gonu moved northwestward striking the gulf countries, Sidr more or less northwards striking Bangladesh and Nargis first west northwestwards and then recurving towards Myanmar coast. Each of them displays different patterns and timeline of development, intensification and decay as well as each of them were driven by different steering currents. Thus, each of them is unique in all the aspects and all of them occurred within a period of 1 year (June 2007–May 2008). These differences in the convective conditions, cyclone basins of genesis and the accuracy of initial and boundary conditions are also reflected in the performance and track errors of the mesoscale models.

It is important to discuss the performance of the driving T254L64 model analyses and forecasts before assessing the mesoscale model. A brief summary of the track error and the errors in the intensity (minimum SLP and maximum wind speed) during the peak intensity period of the tropical cyclone in the T254L64 analysis and forecast is presented in Table 2. It can be seen that Sidr is having maximum track error (394 km) in day-3 forecast though the initial condition has the least error (59 km). The wind speed is grossly underpredicted by T254L64 analysis and forecast in all cases, and especially in the case of Gonu. The large difference in the errors in the minimum SLP between Nargis and Sidr cases is partly due to the difference in the observed intensity between the systems in terms of the dip in the minimum SLP which was not reflected by the global model analyses and forecasts. In other words, the Sidr cyclone (with a minimum SLP of 956 hPa) was more intense than Nargis (with a minimum SLP of 972 hPa) as per the IMD records, whereas T254L64 analysis and prediction produced tropical cyclones with comparable intensity (as obvious from the errors given in the Table 2). Initial locations and strength of the cyclone Gonu have maximum errors. The intensity of Gonu is too underpredicted by the global model, so much so that it cannot be termed as a TC rather than seen as a depression. At the same time, the global model performance of Nargis is the best among the three with its least error in the case of minimum SLP, its correct prediction of a recurving track and the subsequent movement towards Myanmar fairly well in advance. Hence, it can be generally concluded that T254L64 performance was generally better in the case of Nargis than Sidr. When compared with Gonu, though the day-3 track error of Gonu is comparable with the

Table 2 Errors of T254L64 analysis and day-3 forecast in track (km), maximum wind speed (knots) and minimum central pressure (hPa) valid on the day of maximum intensity

TC system (valid day)	Track (Km)		Maximum wind speed (kts)		Minimum pressure (hPa)	
	Analysis	Day-3 fcst	Analysis	Day-3 fcst	Analysis	Day-3 fcst
Nargis (02 May 2008)	115	341	−44.4	−42.7	25.2	25.8
Sidr (15 November 2007)	59	394	−46	−40.3	46.2	41.5
Gonu (05 June 2007)	147.6	300.2	−84	−88.7	64	63.1

Errors are computed from the IMD observations

other two cases, the initial centre location error is much large and the model could not reproduce the intensity of the circulation anyway near the observed in the forecast.

4 Results and discussions

4.1 Track and movement

The WRF NMM model forecast runs are carried out using multiple initial conditions for each case of cyclones as described in Sect. 3. The individual tracks of the cases vary day by day and the forecast positions are also more dependent on the performance of its driving model T254L64 (see Fig. 1). It can be generally observed that the tracks of Nargis lie more or less close to the observed track compared to Gonu and Sidr, where there can be observed more divergence of the directions with each initial conditions and for each convection schemes. To obtain a generalized picture of the track errors, Fig. 2a shows the composites of predicted track errors for each of the tropical cyclone cases across all cumulus parameterization schemes and Fig. 2b for each of the cumulus parameterization schemes across all cases. The composites are computed for each day by averaging track errors from all model runs. It can be seen that KF produces the least errors averaged across all cases, though not much difference is seen on averaging for all the forecast lead times between KF, SAS and GD. Also, BMJ performed poorest among the four when averaged across all the three cases. It can also be seen that Sidr shows the maximum track error followed by Gonu in day-2 and day-3, whereas for day-1 forecasts, there is not much difference in the forecast errors in all the three cases in spite of the fact that Sidr is having the least initial error at $t = 0$.

The poorer track predictions for Gonu and Sidr might be apparently because of the initial location or intensity errors as well as the errors in the tracks predicted by the driving global model. Nargis track predictions are the best among all the three cases in day-2 and day-3, though Sidr has the least mean IC errors. The performance between the four CPSs does not differ much for Nargis case, where the errors in the intensity are the least. It is worth mentioning the fact here that GD failed to predict a strong cyclonic system in many of the instances and the centre itself was not clear enough to locate it, which rules out any fair comparison with the other CPSs.

4.2 Intensity and associated rainfall

When comparing the absolute value of the predicted intensities and the observations, with most of the initial conditions, the mesoscale model grossly underpredicts the same except for KF in the Nargis case. A relative comparison of the intensity and the associated rainfall between the TC cases and the CPSs is attempted in this section. Figure 3 shows the minimum sea level pressure predicted by the four convective schemes, which is a statement of the predicted intensity starting with the same analysis, for Gonu (leftmost column a, d, g and j), Sidr (middle column b, e, h and k) and Nargis (rightmost column c, f, i and l). This shows that in general Gonu was the most underpredicted and Nargis was the best predicted in terms of the intensity. It can be seen that KF is the best in showing a tendency for intensification in the forecasts for Gonu and Sidr cases, whereas for Nargis case, its prediction is more or less matching with the IMD estimates. Among the other three schemes, SAS is the second best, though lagging far behind KF, whereas BMJ and GD fare

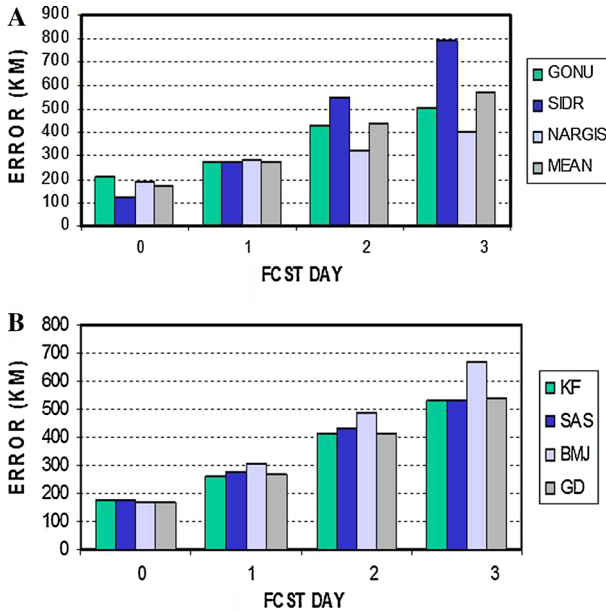


Fig. 2 Composite track errors in kilometers for analysis, day-1, day-2 and day-3 forecasts (a) for Gonu, Sidr and Nargis along with mean error averaged across runs with four CPSs and (b) separately for four CPSs (KF, SAS, BMJ and GD) averaged across all the three systems. Errors are computed from the observed IMD locations

very poor in matching the observed intensity. Exactly similar conclusion can be drawn by the maximum wind speed predicted around the centre of the system (not shown here).

The intensity and the spread of the rainfall produced by the systems on predicted tracks can be estimated by the maximum grid point rainfall accumulated for the previous 24-h period in the corresponding grid boxes in Fig. 4. Figure 5 shows the averaged daily rainfall comparisons with the curves for day-1, day-2 and day-3 forecasts along with the TRMM estimates. KF scheme is seen to produce actually some overprediction of associated rainfall with better input data and initial conditions, like Sidr and Nargis. While for Gonu, it is able to intensify the system so that the rainfall is more or less matching with the observed TRMM estimates. For GD, it is gross underprediction of intensity as well as the associated rainfall for all the cases except Sidr, in which case the associated rainfall in the 10 × 10 degree box is more or less matching with the observed TRMM-derived daily estimates. For Nargis case, the averaged associated rainfall for SAS is a better match with the TRMM estimates, whereas for KF, there is an over intensification and over-prediction. However, it has to be kept in mind while analysing these results that the rainfall associated with the predicted TC is compared with the TRMM rainfall over the same domain, whereas the location of the peak rainfall and the geographical patterns of the observation may be a little bit shifted to those of the forecasts. Thus, only the rainfall captured in the predicted box is used for averaging, and the track-relative analysis and pattern matching is not carried out.

Bias scores (BS), threat scores (TS) and equitable threat scores (ETS) are some of the widely accepted standard parameters for model performance for the categorical measures like rainfall. The rainfall has been divided into 10 different thresholds varying from 1 to 90 mm at 10 mm interval. The verification is done against the TRMM rainfall over the box

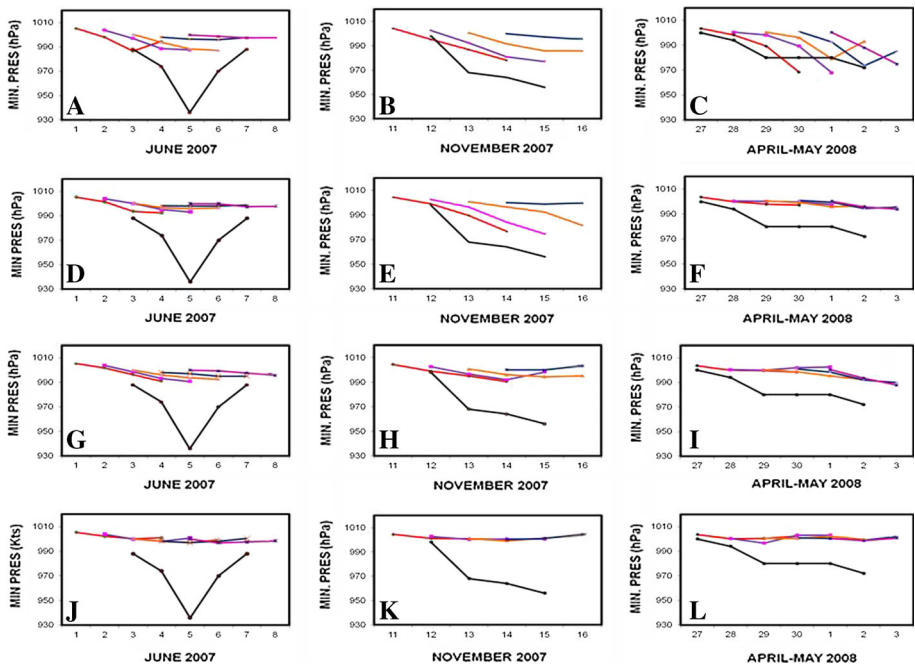


Fig. 3 Minimum central sea level pressures (hPa) in the 10×10 degree box around the predicted centres of TCs by WRF NMM model 3-day runs with different ICs with four CPSs for Nargis (a, d, g, j), Sidr (b, e, h, k) and Nargis (c, f, i, l), along with the IMD observed curves

with the centre of the corresponding forecast run. Figure 6 gives the detailed performance of each physics options for each individual cases averaged across all the forecast lead times of day-1 to day-3, where BS is highest for all the deep convective schemes for Sidr and TS, and ETS scores are much better for Nargis irrespective of the deep convection schemes used. It can be noted that for GD scheme, ETS scores are comparatively highest for Nargis case and lowest for Gonu. In general, GD gives poor results, especially for Gonu in which case the ETS scores are negative.

4.3 Tropical cyclone characteristics

Among the three tropical cyclone cases, Nargis was the best predicted by T254L64 model (in terms of minimum SLP). This is also reflected in the forecast performance by the mesoscale model for all parameterization schemes (in terms of track errors). Figure 7 (Fig. 8) shows the day-2 forecast of 850 hPa geopotential and wind (daily rainfall) valid for 2 May, 2008, for the cyclone Nargis at landfalling stage. (For brevity, the other two cyclone cases are not shown here. See Mohandas and Ashrit (2009) for details). The four panels (a–d) correspond to the four experiments, namely, KF, SAS, BMJ and GD, respectively. The panel e corresponds to T254L64 analysis (TRMM estimates) for geopotential and wind (daily rainfall). KF generally produces the strongest system in terms of intensity and maximum wind speed, whereas GD is the weakest. Similarly, the corresponding rainfall prediction displays the maximum amount of accumulated rainfall predicted by KF, followed by SAS and BMJ, whereas GD shows the least amount of rainfall

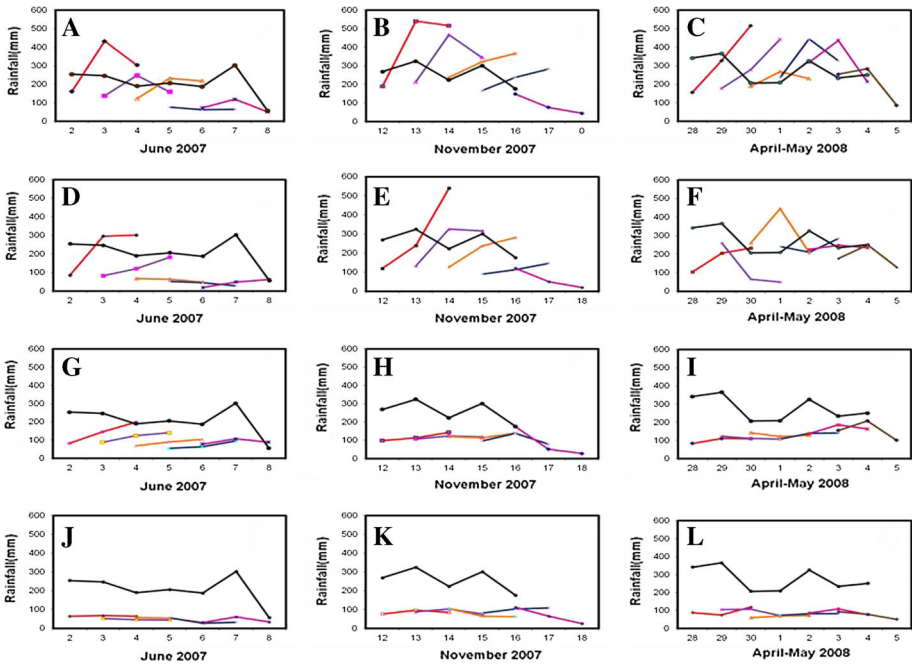


Fig. 4 Similar to Fig. 3, but for maximum previous 24-hour rainfall (mm) in the box area

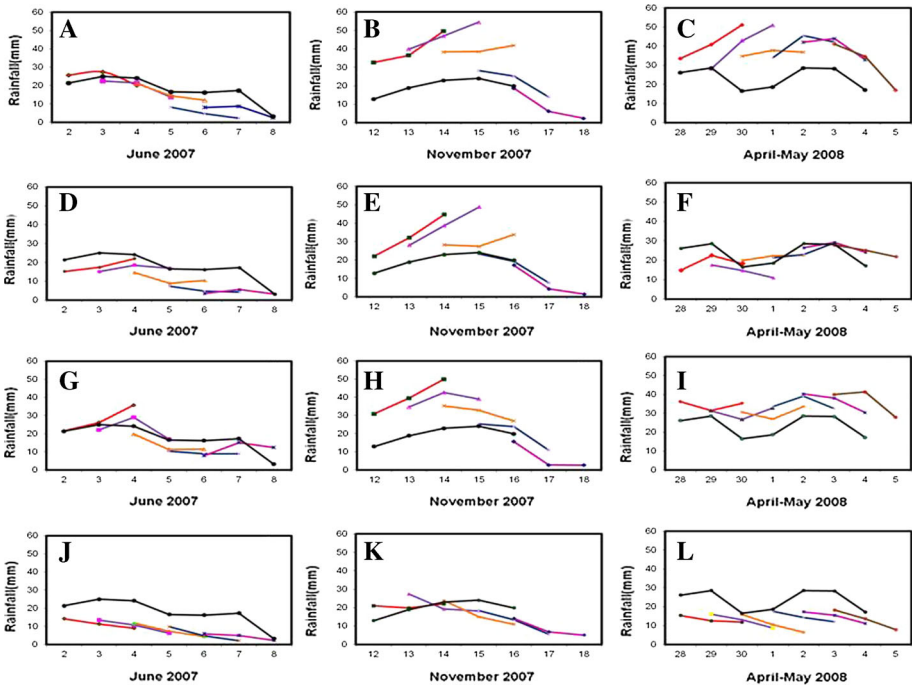


Fig. 5 Similar to Fig. 3, but for previous 24-hour mean rainfall (mm) in the box area

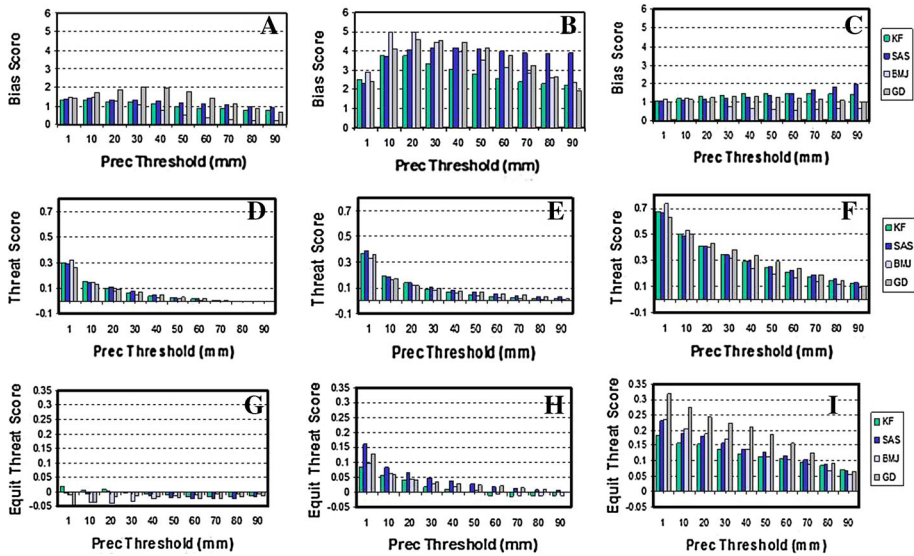


Fig. 6 Bias score (BS), TS and ETS of total rainfall (mm/day) for the thresholds 1, 10, 20, ... 90 mm, and for four CPSs for Gonu (a, d and g), Sidr (b, e and h) and Nargis (c, f and i)

with hardly any contour greater than 8 cms in the case of Nargis, the most intense among the three. Also KF produces the maximum mesoscale variations in the accumulated precipitation values, whereas BMJ and SAS show hardly any mesoscale variability. GD on the other hand, produces too much of spread with patchy light rainfall bands. For Nargis case, though overall the rainfall pattern of BMJ is similar to the TRMM satellite estimates (panel e) even without the associated spatial variability, the location of the maximum rainfall contour is displaced in the forecast.

The analysis of the detailed structure of the TCs requires simulations with mesoscale resolution of the model in the range of a few kilometers. Also the evolution of the narrow eye structure depends not only on the intensity and dimension of the systems, but also on the timing and duration of the mature stage of the development cycle. The three systems under study have different history and characteristics. The peak intensity of the forecasts and the mature stages of its development vary from case to case. Ma and Tan (2009) assess the performance of various CPSs in the simulation of TCs and find some limitations identified in the distribution and intensity of precipitation and the partitioning into grid-resolvable and subgrid-scale components. They found the location and intensity are extremely sensitive to the choice of the cumulus convection. In their study, BMJ tends to overestimate the rainfall coverage and make false alarm of intense rainfall while KF gives the best simulation of TC on the 15-km resolution grids. Grell's scheme tended to underestimate subgrid-scale rainfall due to its deficiency in removing instability. They also suggest that KF can be improved upon for the case of weak synoptic forcing by modification of the triggering mechanism.

An effort has been made to diagnose the relatively large-scale structure of the TCs, by taking vertical cross section of the relative humidity (percentage) around the estimated centre of the system at the forecast time of the maximum intense or mature stage of development as simulated by the Nargis case valid for 2 May, 2008, in Fig. 9 for the four deep convective schemes KF, SAS, BMJ and GD, respectively. Also the horizontal extent

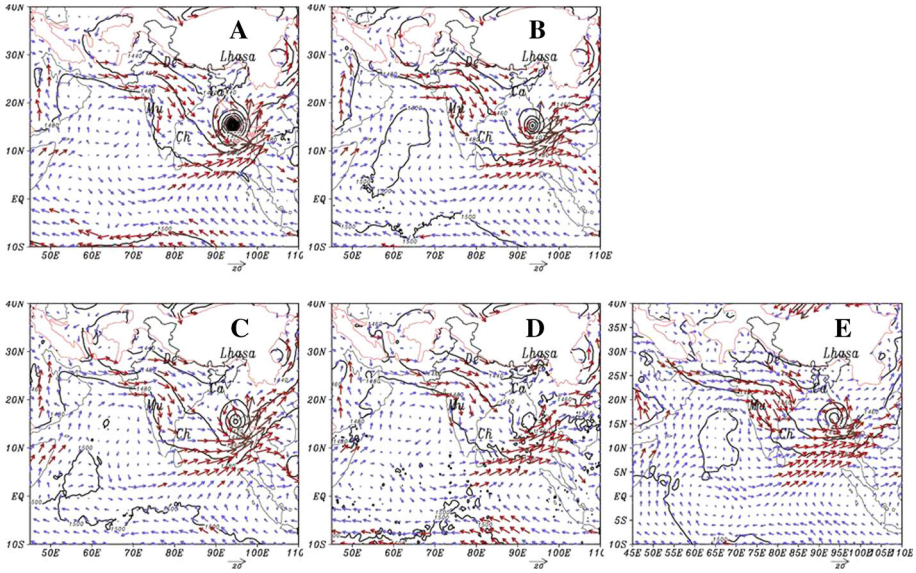


Fig. 7 Geopotential (m) contours and wind (m/s) arrows for the day-2 forecast valid for 02 May, 2008, using WRF NMM model with CPSs a KF, b SAS, c BMJ and d GD, along with e T254L64 verifying analysis

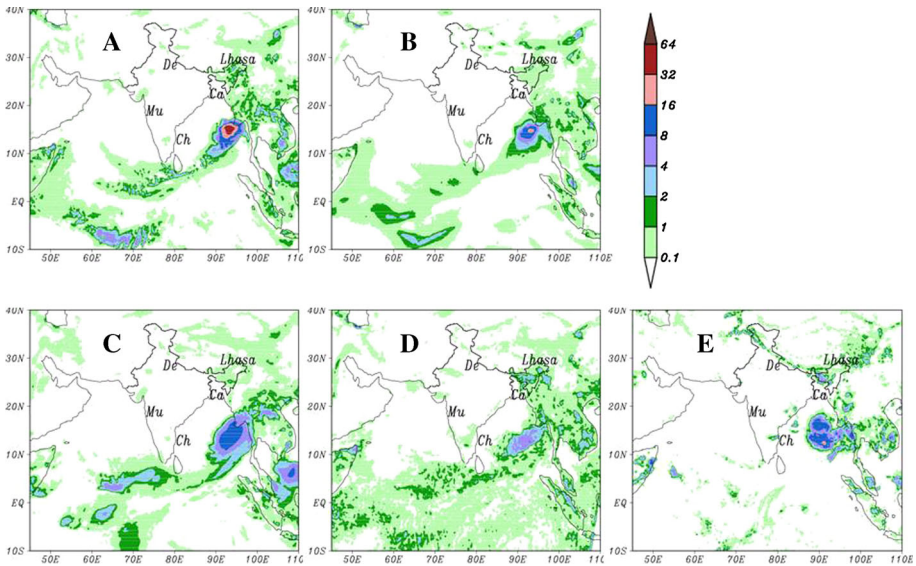


Fig. 8 Similar to Fig. 7 for panels (a–d), but for previous 24-h accumulated rainfall (cm- shading) valid at 00Z 02 May, 2008 and along with e TRMM 3B42RT-derived daily rainfall estimates

of relative humidity (RH-percentage) and vertical velocity (Pascal per second) in the 10×10 degree box surrounding the estimated centre locations in the forecasts corresponding to the four deep convective schemes are also shown in Figs. 10 and 11 respectively. The circulation vectors shown in the figures are those corresponding to the vertical

or horizontal planes, as the case is. Also Figs (12, 13) show the distribution of total precipitation (APCPSFC) and non-convective part (NCPCPSFC) corresponding to the four deep convective schemes.

When compared with the vertical extent of the strong updraft and the humid air into the upper troposphere, KF outcores all other schemes with a stronger updraft near the cyclonic centre spreading over in the upper levels in the shape of a funnel and with a relatively dry middle troposphere (Fig. 9). When comparing the distribution of RH at 850 hPa level as shown in Fig. 10, KF shows maximum vertical organization with the same initial and boundary conditions, whereas all other schemes produce relatively shallow humid layer spreading over more horizontal extent particularly with GD the humid layer being very thin in the lower layers. From this distribution of RH, it can be easily assumed that KF and SAS produced the maximum convective organization and hence the humidity in the lower troposphere generating significant rainfall associated with the system, compared to BMJ and GD with its weaker convective organization.

Figure 11 shows that KF produced a narrow region of updraft near the centre with stronger downdrafts dominating the surroundings, whereas GD shows predominantly weaker updraft and downdraft cells spread over the box. It can be seen from Figs. 12 and 13 that only KF and SAS produce a component of non-convective rainfall, whereas BMJ

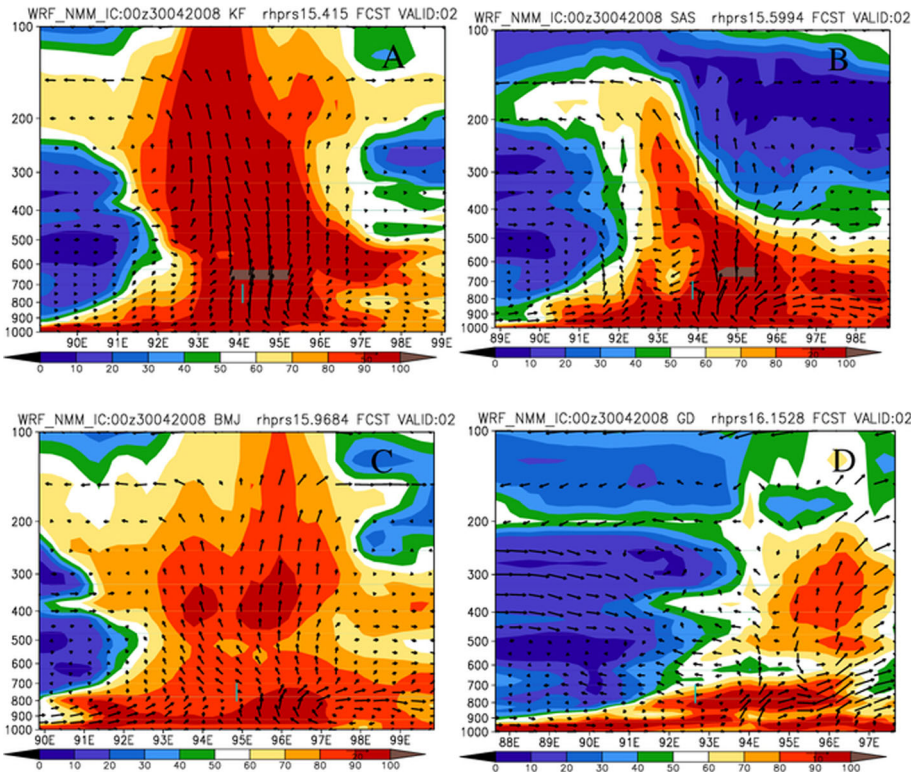


Fig. 9 The vertical cross sections of relative humidity (%age—shaded) along the predicted latitudes by WRF NMM models with vertical wind vectors (m/s) for four CPSs KF (a), SAS (b), BMJ (c) and GD (d), valid for 02 May, 2008

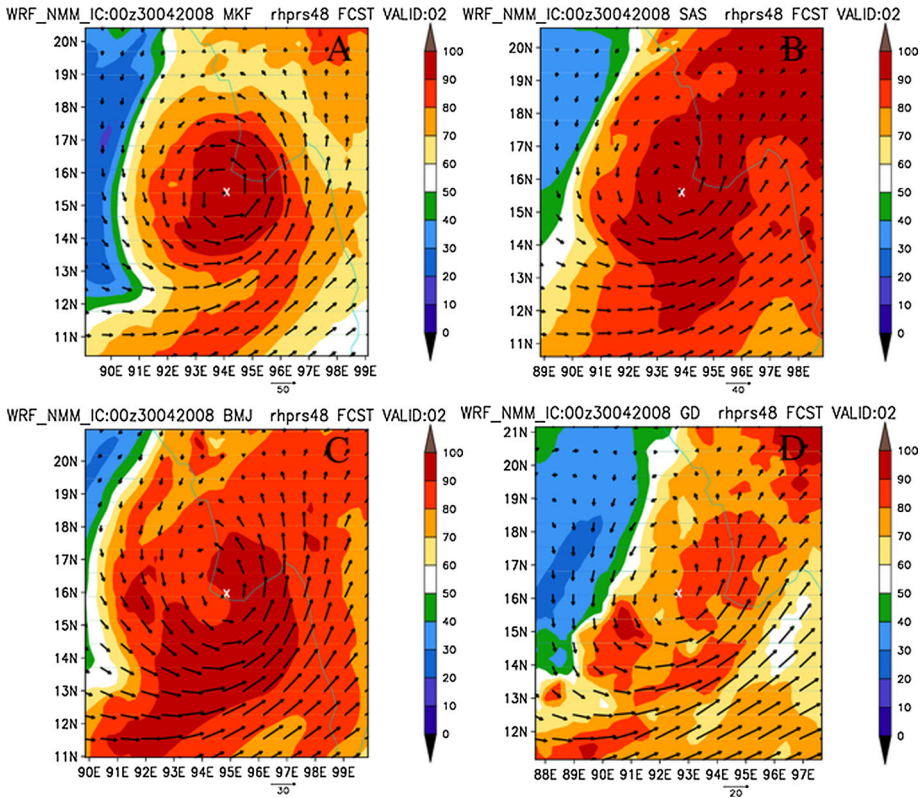


Fig. 10 Distribution of relative humidity (%age—shaded) at 850 hPa level in the grid box centred around the predicted locations of TC with four CPSs KF (a), SAS (b), BMJ (c) and GD (d), along with the horizontal wind vectors (m/s)

and GD generate almost entire amount of its rainfall from the deep convective scheme. KF showed maximum organization, stronger updrafts and downdrafts and precipitation, and GD showed the least organization and precipitation with the smaller cells of weaker vertical air motions filled over the entire box which is apparently dissipating the total energy over the domain. These differences may be mainly coming from the characteristics of the deep convective parameterization schemes used for the forecast runs and its interaction with the other model physics components.

Although the results are shown only for Nargis case in Figs. 9, 10, 11, 12 and 13, the similar analyses are made for Gonu and Sidr cases (figures not shown). The quality of initial and boundary conditions prevents conclusive verification of cyclone Gonu. It can be broadly stated that none of the schemes produced observed peak intensity. Generally intensity forecasts for all fields produced for Gonu by all the deep convective schemes are weaker compared to Sidr and Nargis. For Sidr and Nargis cases, only KF and SAS produced some component of grid-scale rainfall, whereas BMJ and GD produced no significant amount of the same for any of the three cases. This implies that, at this resolution for tropical cyclone cases, the moisture processes in BMJ and GD parameterization schemes behave in a manner so that almost the entire precipitation is produced by the subgrid scale. For KF, and under strong convective conditions for SAS also, the deep convection scheme

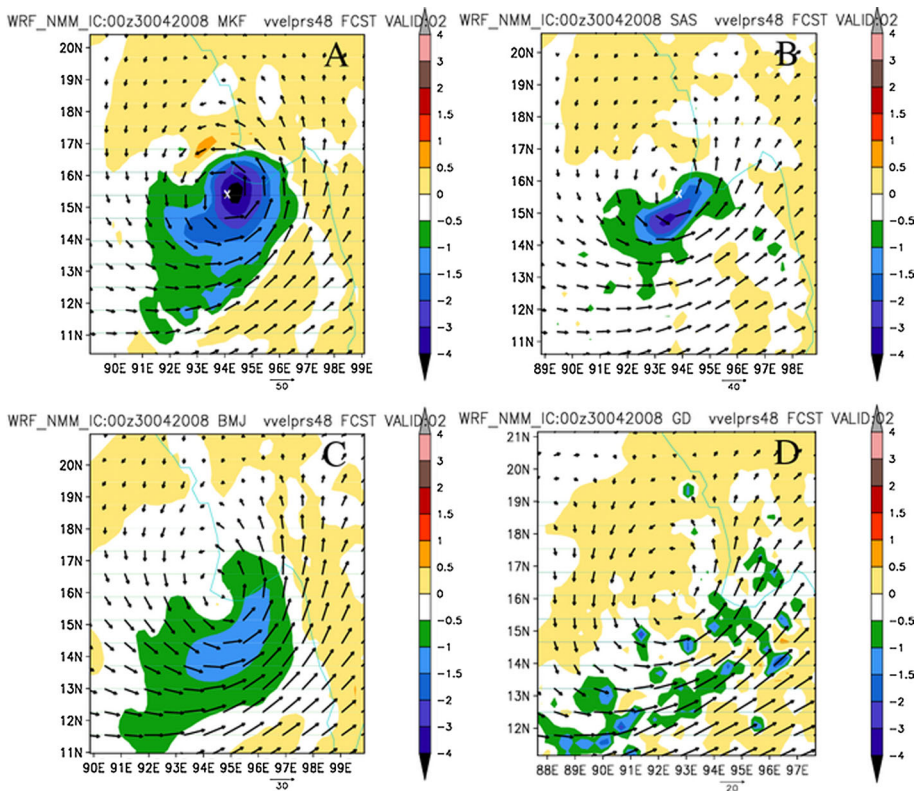


Fig. 11 Similar to Fig. 10, but for omega (Pa/s) at 850 hPa level

leaves the grid points more moist, which may lead to super saturation at the grid points and which in turn eventually rains out as the large-scale precipitation. The vertical cross section of relative humidity also throws some light on the differences in the behaviour of the CPSs with respect to different convective environments associated with the three cases. KF always tends to have strong vertical updraft near the centre and invariably pumps in moisture to higher and higher levels, causing more grid-scale condensation even in the case of relatively weak convective environment associated with the initial conditions for TC Gonu. SAS could not produce any moist updraft which might have resulted into insignificant grid-scale rain in the case of Gonu, while for Sidr and Nargis, it did produce some grid-scale component. For BMJ and GD, virtually there is no vertical mixing and hence produced very shallow layers of moist air resulting into lesser contribution from the non-convective part. Other major difference in the behaviour of CPSs across all the cases is the apparent single tower-like structure of humidity buildup for KF in contrast to double tower structure on the either side of the centre for BMJ. SAS shows a combination of both varying with case to case, and GD shows no organized buildup. Generally, it can be observed from the horizontal distributions of rainfall fields that the concentrations of convective activity is to the northeast, south and southwest of cyclonic centre for Gonu, Sidr and Nargis, respectively.

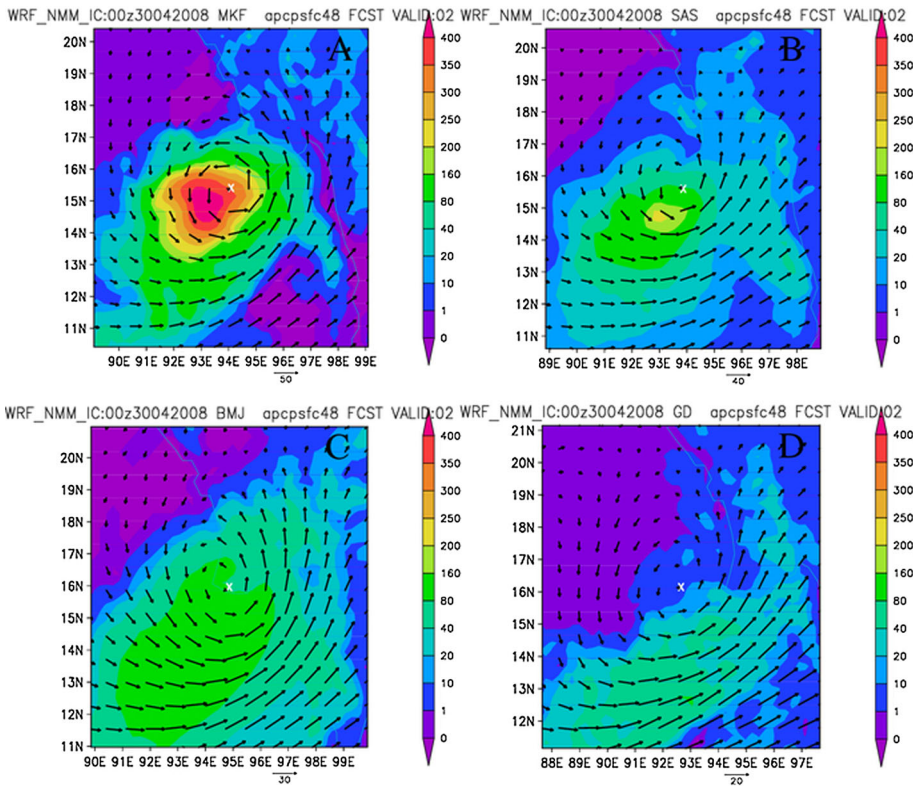


Fig. 12 Total precipitation (mm/day) for the box areas corresponding to the predicted centres of TCs by WRF NMM with four CPSs (a-d respectively) valid for day-2 forecasts at 00Z 02 May, 2008

5 Discussion

In general, it can be stated that KF produces the strongest intensity and GD features the weakest intensity. The experiments using SAS and BMJ feature intermediate intensification. Similarly, KF produces the highest amount of associated rainfall and convective organisation, while GD produces the least rainfall amount failing to capture the cyclone evolution and intensification. GD produces only a broad, diffused and a weak cyclone structure. As a result, GD produces only the rainfall in the feeder bands to the south of the cyclone position. Also it can be noted that for the cases with weaker convective forcings or with initial and boundary conditions having poor intensity and greater positional errors, like that of Gonu, there is large difference in the behaviour of the cumulus parameterization schemes as well as its feedbacks with the surrounding environment. In contrast to that, for the cases with strong convective forcings as provided by the driving global model, like the case of Nargis, the performance of the various deep convection schemes are more or less similar. This is in agreement with the observations by Yang and Tung (2003) that for the cases with strong synoptic forcings, the synoptic or mesoscale environment provides the primary control on the model’s rainfall forecast skill, and the CPSs used in the model only slightly modify forecasts.

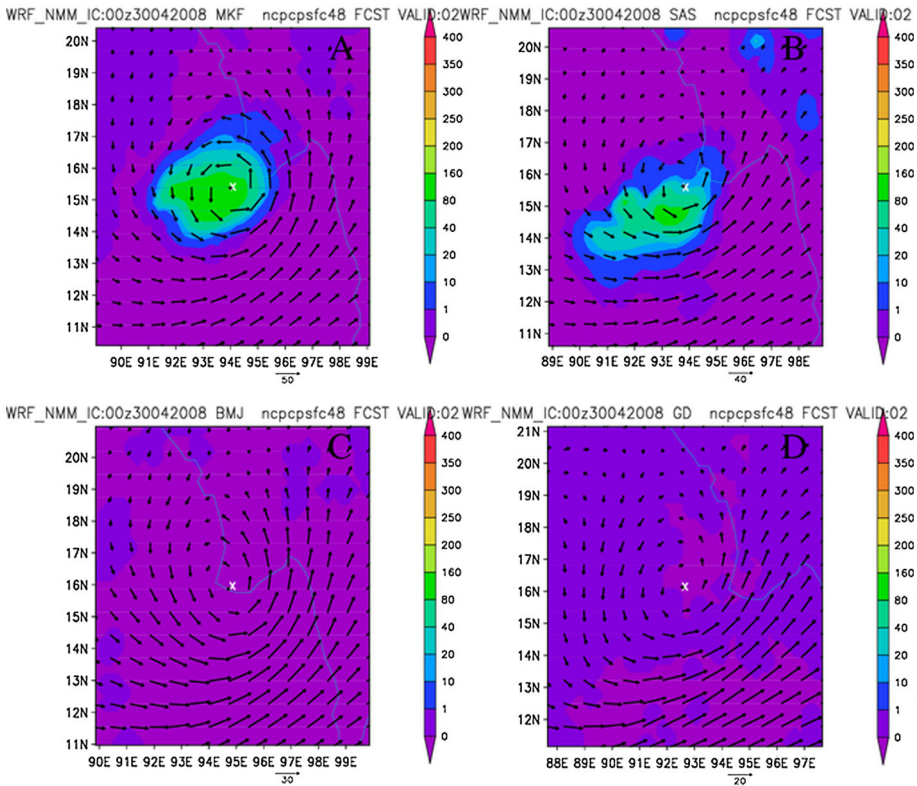


Fig. 13 Similar to Fig. 13, but non-convective precipitation (mm/day)

The differences in the convective conditions and the quality of initial and boundary conditions notwithstanding, there can be observed a clear-cut variability and other characteristics associated with the performance of the various deep convective physics options employed in the mesoscale models. The diagnosis of the reasons for these behaviour patterns of the deep convection schemes in the different scenarios requires much deeper analysis and sensitivity studies and is beyond the scope of this study. However, one aspect of the so called cumulus parameterization problem lies in the representation of both resolved and subgrid-scale precipitation processes and its dependency on the model resolution (Frank 1983). Wang and Seaman (1997) reported following a very detailed study that the rainfall partitioning into subgrid scale and grid scale is sensitive to the particular parameterization scheme chosen, but relatively insensitive to the model resolution as well as the convective environments. The implicit and explicit schemes operate simultaneously in the model to represent both the subgrid-scale and resolvable-scale (mesoscale) precipitation processes. Zhang (1989) show that this approach will handle mixed convective and stratiform precipitation systems and does not double count the effects of either resolvable-scale or subgrid-scale heating and moistening.

Figure 14 shows the percentage ratio of non-convective to total rainfall averaged for all forecast period along with the mean total daily precipitation averaged across all the cases as well as across all the physics experiments. It is evident that KF produced maximum total rainfall followed by BMJ, SAS and GD with GD producing only about one-third quantity

of KF rainfall amount as a whole. KF and SAS produced more fraction of precipitation of grid scale to the total precipitation (10–14 %), whereas BMJ and GD produced very negligible fraction (up to about 2 %). It is to be noted that though there is not much difference between Sidr and Nargis in the total as well as the grid-scale fraction of precipitation, there seems to be a significant reduction in the total as well as the fractional rainfall production for Gonu. Wang and Seaman (1997) stated that the differences in the convective to total precipitation ratio between the CPSs may be related to the precipitation efficiency parameter and the closure assumptions. They dismissed any significant sensitivity of the model horizontal resolution also, on the partition of precipitation generated between convective and explicit processes. However, as the different CPSs are formulated and tested for some particular rainfall events and at different resolutions, more detailed case studies at different resolutions and under different convective conditions are required for each of the CPSs before any conclusive statement can be made.

6 Summary

Purpose of this study is not strictly to evaluate the CPSs or the individual cases with respect to the observations, but to compare characteristic responses and errors associated with the CPSs and with respect to some particular synoptic and convective conditions. Thus, the order of track errors and average parameters of the forecast runs with respect to the observation, though shown for comparisons, is slightly higher when averaging across all cases or all CPSs. Also the verification is not done for the entire integration domain, but only for a square grid box of each side 10 degrees in length assuming that this area covers most of the associated features with respect to the particular TC under study. This may be

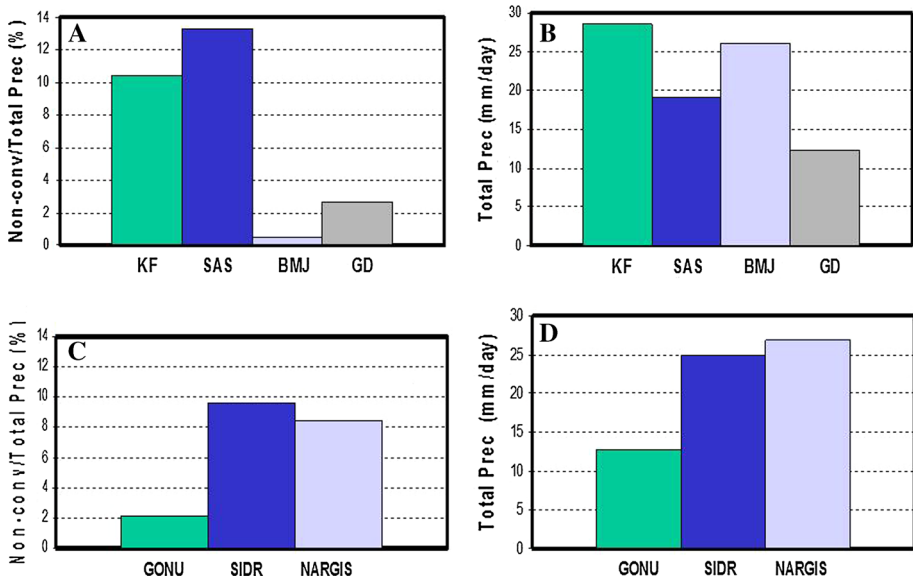


Fig. 14 Percentage ratio of non-convective to total precipitation (a and c) along with mean total precipitation (b and d) in mm/day for 4 CPSs averaged across all cases (a and b) and across all CPSs (c and d)

another reason contributing to the relatively higher order of errors in statistical parameters compared to other studies as this region of associated rainfall may not entirely coincide with the region of actual rainfall as estimated by the TRMM estimates which are probably the best source of derived rainfall over oceanic regions. So the emphasis has been given to the relative comparison between CPSs or cases rather than the absolute value of the parameters.

Generally it is known that part of the forecast errors depends on the physics, initial and boundary conditions and the synoptic/convective conditions, like the region of formation, data availability to represent the actual pattern and intensity of the TC, accuracy and mesoscale details in initial conditions and the accuracy of the lateral boundary conditions as in this case, and the performance of the global model forecasts to which the WRF NMM is nested. These external parameters are identical for all CPSs for each case but relevant in casewise comparison. Thus, the present study is not only the comparison of CPSs, but also on the effect of the synoptic/convective conditions pertaining to each of the TC history. Track and intensity of the three cases chosen vary with the physics as well as the geographically related factors. The three cases are unique examples and the forecast performances, and hence, the impact varies in each case. Sidr shows the maximum track error followed by Gonu in day-2 and day-3, and Nargis shows the least. Also comparison of track errors shows that KF produces the least errors averaged across all cases, though not much difference is seen on averaging for all the forecast lead times between KF, SAS and GD. BMJ performed poorest among the four when averaged across all the three cases.

Intensity and associated rainfall also vary from case to case with Nargis producing most intense patterns, KF trying to slightly over-predict the intensity and GD giving the least performance. Gonu failed to produce the observed intensity and the associated rainfall. KF shows a tendency to overpredict the peak gustiness in the spiral bands with the forecast lead time and produced the strongest convective organization, stronger and narrow region of the updraft and deepest moist troposphere in a column around the cyclonic centre, followed by SAS. GD in fact shows the weakest organization and spreading of energy over a large area and thus dissipates faster being unable to sustain the intensity. The standard rainfall verification scores also show a consistently better performance by the KF scheme. However, it can be seen that the sensitivity of model forecasts is equal or more to the external factors and convective conditions than the sensitivity between the CPSs itself. This is also at least partially applicable to the partitioning of the total precipitation into convective as well as grid-scale fractions. In general, KF and SAS were found to be more efficient than BMJ and GD, while Gonu being least efficient compared to Sidr and Nargis. Thus, while evaluating the performance of the mesoscale models, one should keep in mind the convective environments and the quality of initial and boundary conditions provided to the model. Many studies have shown sensitivity of cumulus convection to the location and intensity of the circulation and associated rainfall, and to the partition of grid-scale and subgrid-scale precipitation. A main feature which can be noticed is that KF and SAS produce more fraction of grid-resolvable component of precipitation, whereas BMJ and GD produce very negligible fraction. This feature may be more sensitive to the specific details of the CPSs, like convective trigger criteria and closure assumptions employed in the respective schemes, as compared to the synoptic or convective conditions.

The study also reaffirms the conclusion from other studies over other synoptic conditions, other basins and other rainfall events that, in general, most of the CPS performances will not vary much under strong synoptic forcings. The synoptic environment is input into the model through the initial and lateral boundary conditions from the global model. Also the synoptic environment provided by global models may not always be close to reality as

it depends on the accuracy and performance of the global model system itself, which in turn depends partly on the quality and quantity of the data over the oceanic basin of TC genesis. As in the case of Gonu, the initial condition itself lacked the strong convective conditions over the Arabian Sea basin, without which the model might not have generated a tendency to produce strong vertical motions so as to break the inversion conditions predominant in the Arabian Sea. There can be a wide range of performance variations and feedbacks under weak synoptic forcings. Part of the precipitation forecast errors does not result directly from a given CPS or model deficiencies, but may be related to uncertainties in the model's initial conditions. The quality of the initial condition can be very important for good precipitation forecasts, especially when the large-scale dynamic forcing is weak. At a resolution of about 27 km, KF is found to be the best among the CPSs as far as TCs over Indian Ocean basin are concerned, in simulating the near-realistic observed intensity. This conclusion cannot be generalized for all resolutions, all the TC cases or all other basins, but many examples of recent studies have thrown up similar conclusions. Also it cannot be stated that any single CPS can be identified to perform better in all types of rainfall events or convective conditions.

Acknowledgments Global and mesoscale models mentioned in this study are adopted versions from National Centre for Environment Prediction (NCEP), USA. Rainfall observations are derived daily TRMM precipitations, and observed tracks of the three tropical cyclone cases are obtained from India Meteorological Department (IMD). The authors are thankful to the two anonymous reviewers for their constructive comments in greatly improving the manuscript.

References

- Akter N, Tsuboki K (2012) Numerical simulation of cyclone Sidr using a cloud-resolving model: characteristics and formation process of an outer rainband. *Mon Weather Rev* 140:789–810
- Arakawa A, Schubert WH (1974) Interaction of a cumulus cloud ensemble with the large-scale environment, part I. *J Atmos Sci* 31:674–701
- Aylward RD, Dyer JL (2010) Synoptic environments associated with the training of convective cells. *Weather Forecasting* 25:446–464
- Belanger JI, Webster PJ, Curry JA, Jelinek MT (2012) Extended prediction of north Indian ocean tropical cyclones. *Weather Forecasting* 27:757–769
- Betts AK, Miller MJ (1993) The Betts–Miller scheme. In: The representation of cumulus convection in numerical models. *Meteor Monogr No 46*, Amer Meteor Soc, pp 159–164
- Chen T-C, Tsay J-D, Yen M-C, Cayan EO (2010) Formation of the Philippine twin tropical cyclones during the 2008 summer monsoon onset. *Weather forecasting* 25:1317–1341
- Chen G, Xue H, Zhang W, Zhou X (2012) The three-dimensional structure of precipitating shallow cumuli. Part one: the kinematics. *Atmos Res* 112:70–78
- Cram JM, Pielke RA, Cotton WR (1992) Numerical simulation and analysis of a prefrontal squall line. Part I: observations and basic simulation results. *J Atmos Sci* 49:189–208
- Davis C, Wang W, Dudhia J, Torn R (2010) Does increased horizontal resolution improve Hurricane wind forecasts? *Weather Forecasting* 25:1826–1841
- Deb SK, Srivastava TP, Kishtawal CM (2008) The WRF performance for the simulation of heavy precipitating event over Ahmedabad during August 2006. *J Earth Sys Sci* 117:589–602
- Deb SK, Kishtawal CM, Pal PK (2010) Impact of Kalpana—I derived water vapour winds on Indian Ocean tropical cyclone forecasts. *Mon Weather Rev* 138:987–1003
- Dudhia J (1989) Numerical study of convection observed during the winter monsoon experiment using a mesoscale two-dimensional model. *J Atmos Sci* 46:3077–3107
- Evan AT, Camargo SJ (2011) A climatology of Arabian sea cyclonic storms. *J Clim* 24:140–158
- Frank WM (1983) The cumulus parameterization problem. *Mon Weather Rev* 111:1859–1871
- Gallus WA Jr (1999) Eta simulations of three extreme precipitation events: sensitivity to resolution and convective parameterization. *Weather Forecasting* 14:405–426

- Gentry MS, Lackmann GM (2010) Sensitivity of simulated tropical cyclone structure and intensity to horizontal resolution. *Mon Weather Rev* 138:688–704
- Gopalakrishnan SG, Goldenberg S, Quirino T, Zhang X, Marks F, Yeh K-S, Atlas R, Tallapragada V (2012) Toward improving high resolution numerical hurricane forecasting: influence of model horizontal grid resolution, initialisation and physics. *Weather Forecasting* 27:647–666
- Gray WM (1968) Global view of the origin of tropical cyclones and storms. *Mon Weather Rev* 96:669–700
- Grell GA (1993) Prognostic evaluation of assumptions used by cumulus parameterizations. *Mon Weather Rev* 121:764–787
- Grell GA, Devenyi D (2001) Parameterized convection with ensemble closure/feedback assumptions. In: *Proceedings of 9th conference on Mesoscale processes*. Amer Meteor Soc, July 30–August 2, 2001, Ft Lauderdale, pp 12–16
- Grell GA, Devenyi D (2002) A generalized approach to parameterizing convection combining ensemble and data assimilation techniques. *Geoph Res Lett* 29, NO 14
- Grell GA, Dudhia J, Stauffer DR (1994) A description of the fifth generation Pen State/NCAR Mesoscale Model (MM5). NCAR Tech Note NCAR/TN-398 + STR
- Houze RA Jr (1977) Structure and dynamics of a tropical squall line system. *Mon Weather Rev* 105:1541–1567
- Houze RA Jr (1997) Stratiform precipitation in region of convection: a meteorological paradox? *Bull Amer Meteor Soc* 78:2179–2196
- Janjic ZI (1994) The step-mountain eta coordinate model: further developments of the convection, viscous sublayer and turbulence closure schemes. *Mon Weather Rev* 122:927–945
- Janjic ZI (2000) Comments on “development and evaluation of a convective scheme for use in climate models”. *J Atmos Sci* 57:3636
- Johnson RH, Hamilton PJ (1988) The relationship of surface pressure features to the precipitation and air flow structure of an intense midlatitude squall line. *Mon Weather Rev* 116:1444–1472
- Kain JS (2004) The Kain–Fritsch convective parameterization: an update. *J Appl Meteor* 43:170–181
- Kain JS, Fritsch JM (1990) A one-dimensional entraining/detraining plume model and its application in convective parameterization. *J Atmos Sci* 47:2784–2802
- Kain JS, Fritsch JM (1993) Convective parameterization for mesoscale models: The Kain-Fritsch scheme. In: *The representation of cumulus convection in numerical models*. Meteor Monogr No. 24, Amer Meteor Soc, pp 165–170
- Krikken F, Steenveld GJ (2012) Modelling the re-intensification of tropical storm Erin (2007) over Oklahoma: understanding the key role of downdrafts formulation. *Tellus A* 64:17417. doi:[10.3402/tellusa.v64i0.17417](https://doi.org/10.3402/tellusa.v64i0.17417)
- Kuo Y-H, Reed RJ, Liu Y (1996) The ERICA IOP 5 storm, part III: mesoscale cyclogenesis and precipitation parameterization. *Mon Weather Rev* 124:1409–1434
- Lisan Y, McPhaden MJ (2011) Ocean precondition of cyclone Nargis in the Bay of Bengal: interaction between Rossby waves, surface fresh waters and sea surface temperatures. *J Phys Oceanogr* 41:1741–1755
- Litta AJ, Idicula SM, Mohanty UC (2011) A comparative study of convective parameterization schemes in WRF–NMM model. *Int J Comp Appl* 33:32–40
- Ma L-M, Tan Z-M (2009) Improving the behavior of the cumulus parameterization for tropical cyclone prediction: convection trigger. *Atmos Res* 92:190–211
- Marchok T, Rogers R, Tuleya R (2007) Validation schemes for tropical cyclones quantitative precipitation forecasts: evaluation of operational models for US land falling cases. *Weather Forecasting* 22:726–746
- Mohandas S, Ashrit R (2009) Tropical cyclone prediction using different convective parameterization schemes in a mesoscale model. NCMRWF research report NMRF/RR/1/2011, NCMRWF (Min Earth Sciences), A-50, Sector-62, Noida, June 2011
- Molinari J, Dudek M (1992) Parameterization of convective precipitation in mesoscale numerical models: a critical review. *Mon Weather Rev* 120:326–344
- Nasrollahi N, AghaKouchak A, Li X, Hsu K, Sorooshian S (2012) Assessing the impacts of different WRF precipitation physics in hurricane simulation. *Weather Forecasting* 27:1003–1016
- Pan H-L, W-S Wu (1995) Implementing a Mass Flux Convection Parameterization Package for the NMC Medium-Range Forecast Model. NMC Office Note No 409. [Available from NCEP, 5200 Auth Road, Washington, DC 20233]
- Peng X, Tsuboki K (1997) Impact of convective parameterizations on mesoscale precipitation associated with the Baiu front. *J Meteor Soc Japan* 75:1141–1154
- Rafy ME, Hafez Y (2008) Anomalies in meteorological fields over northern Asia and its impact on hurricane Gonu. In: *Proceedings of 28th conference on hurricanes and tropical meteorology*, Amer Meteor Soc, 28April–2 May 2008, Orlando, FL

- Rajagopal EN, Das Gupta M, Mohandas S, George JP, Iyengar GR, Kumar DP (2007) Implementation of T254L64 global forecast system at NCMRWF. NCMRWF technical report NMRF/TR/1/2007, NCMRWF (Min Earth Sciences), A-50, Sector-62, Noida, May 2007
- Rao DVB, Prasad DH (2007) Sensitivity of tropical cyclone intensification to boundary layer and convective processes. *Nat Hazards* 41:429–445
- Roy C, Kovordanyi R (2012) Tropical cyclone track forecasting techniques—a review. *Atmos Res* 104–105:40–69
- Schumacher RS, Johnson RH (2005) Organisation and environmental properties of extreme rain producing mesoscale convective systems. *Mon Weather Rev* 133:961–976
- Simpson JS, Kummerow C, Tao W-K, Adler RF (1996) On the tropical rainfall measuring mission (TRMM). *Meteorol Atmos Phys* 60:19–36
- Singh AP, Singh RP, Raju PVS, Bhatla R (2011) The impact of three different cumulus parameterization schemes on the Indian summer monsoon circulation. *Int J Ocean Clim Syst* 2:27–44
- Spencer PL, Stensrud DJ (1998) Simulating flash flood events: importance of the subgrid representation of convection. *Mon Weather Rev* 126:2884–2912
- Stensrud DJ, Fritsch JM (1994) Mesoscale convective systems in weakly forced large-scale environments, part III: numerical simulations and implications for operational forecasting. *Mon Weather Rev* 122:2084–2104
- Stensrud DJ, Bao J-W, Warner TT (2000) Using initial conditions and model physics perturbations in short-range ensemble simulations of mesoscale convective systems. *Mon Weather Rev* 128:2077–2107
- Vaidya SS (2007) Simulation of weather systems over Indian region using mesoscale models. *Meteorol Atmos Phys* 95:15–26
- Vaidya SS, Kulkarni JR (2007) Simulation of heavy precipitation over Santacruz, Mumbai on 26 July 2005, using mesoscale model. *Meteorol Atmos Phys* 98:55–66
- Wang Z (2012) Thermodynamic aspects of tropical cyclone formation. *J Atmos Sci* 69:2433–2451
- Wang W, Seaman NL (1997) A comparison study of convective parameterization schemes in a mesoscale model. *Mon Weather Rev* 125:252–278
- Yang M-J, Tung Q-C (2003) Evaluation of rainfall forecasts over Taiwan by four cumulus parameterization schemes. *J Meteorol Soc Japan* 81:1163–1183
- Yang M-J, Chien F-C, Cheng M-D (2000) Precipitation parameterizations in a simulated Mei-Yu front. *Terr Atmos Oceanic Sci* 11:393–422
- Zhang D-L (1989) The effect of parameterized ice microphysics on the simulation of vortex circulation with a mesoscale hydrostatic model. *Tellus* 41A:132–147
- Zhang D-L, Gao K, Parsons DB (1989) Numerical simulation of an intense squall line during 10–11 June 1985 PRE-STORM. Part I: model verification. *Mon Weather Rev* 117:960–994
- Zheng Y, Xu Q, Stensrud DJ (1995) A numerical simulation of the 7 May 1985 mesoscale convective system. *Mon Weather Rev* 123:1781–1799